A Three dimensional Transient Two-Phase Flow Analysis with a Density Pertubation Finite Volume Method

Marc Grandotto, Julien Cortes

A Three dimensional Transient Two-Phase Flow Analysis with a Density Pertubation Finite Volume Method

Marc Grandotto * Julien Cortes [1]

French Atomic Energy Commission (CEA), Centre de Cadarache , France

Abstract

In this paper we present the analysis of a full three dimensional transient two-phase flow with strong desequilibria. This analysis uses a finite volume scheme with a density perturbation method recently developed. The application test case is a three dimensional extension of a one dimensional experiment on blowdown pipe. The results are stable with mesh refinements and show realistic three dimensional effects.

Key words: Two-phase flows, Finite volume method, Numerical benchmark tests, Three space dimensions

PACS:

* CEA/DEN/DTP/STH/LTA, Centre de Cadarache, 13108 St Paul lez Durance
Email addresses: mgrandotto@cea.fr (Marc Grandotto),

julien.cortes@fr.thalesgroup.com (Julien Cortes).

[1] presently at Thales Systemes Aeroportes

1 Introduction

The study of real three dimensional transient two-phase flows (liquid and gas) is of first interest in many industrial areas such as petroleum and nuclear applications. The improvments in numerical methods and the growing computer power avalaible should allow to make such studies. But experimental results are needed to test the numerical schemes. There exists several experimental or analytical references in one dimension but few in two dimension [14] and very few in three dimension. We can nevertheless refer also to the works presented in the following references [7] [8] [9].

The purpose of this paper is to investigate a transient two-phase flow in a bended pipe during a pressure blowdown. Pressure blowdowns occur in the primary coolent loops of the pressurized water nuclear reactors when a pipe breaks suddenly. It is considered as a reference accident because it can lead to nuclear core damages due to the lost of the coolent flow. For these reasons this situation has been experimentaly investigated [13]. Only one dimensional analysis have been done due to the difficulties presented by such flows : fast phase change transients at high pressure (several tens bars). We propose in this paper a numerical simulation of a three dimensional extension of this one dimensional situation : bended pipes actually exist in the coolent loops and these geometries imply real three dimensional effects that are not present in one dimension. As we do not have yet similar experimental measurements for this situation, the results are analysed using a space constistency point of view and considering their physical coherence.

The numerical method used in this work is based on the density perturbation method presented in [3][4].

The section 2 presents the governing equations. The section 3 gives the three dimensional system to be solved. The section 4 recall the numerical method. And in the section 5 the results of the three dimensional application are detailed .

2 Governing equations

2.1 The basic conservation equations

The two-fluid model can be written in the general form ([5][6]) (∂_t is the time derivative, $\nabla.$ is the divergence operator and ∇ is the gradient operator) :

- **mass conservation equation :**

$$\partial_t(\alpha_k\rho_k) + \nabla.(\alpha_k\rho_k\overrightarrow{V_k}) = \Gamma_k \,, \tag{1}$$

- **momentum conservation equation :**

$$\begin{gathered}\partial_t(\alpha_k\rho_k\overrightarrow{V_k}) + \nabla.(\alpha_k\rho_k\overrightarrow{V_k}\otimes\overrightarrow{V_k}) + \alpha_k\nabla p_k + \\ (p_k - p_k^i)\nabla\alpha_k = \overrightarrow{F_k^i} + \alpha_k\rho_k\overrightarrow{g} + \Gamma_k\overrightarrow{V_k^i} \,,\end{gathered} \tag{2}$$

- **energy conservation equation :**

$$\begin{gathered}\partial_t(\alpha_k\rho_k(e_k + \tfrac{\overrightarrow{V_k}.\overrightarrow{V_k}}{2})) + \nabla.(\alpha_k\rho_k(h_k + \tfrac{\overrightarrow{V_k}.\overrightarrow{V_k}}{2})\overrightarrow{V_k}) + p_k\partial_t\alpha_k + \\ (p_k - p_k^i)\nabla\alpha_k.\overrightarrow{V_k^i} = Q_k^i + \overrightarrow{F_k^i}.\overrightarrow{V_k^i} + \alpha_k\rho_k\overrightarrow{g}.\overrightarrow{V_k} + \Gamma_k(h_k^i + \tfrac{\overrightarrow{V_k^i}.\overrightarrow{V_k^i}}{2}) \,,\end{gathered} \tag{3}$$

where the subscript k refer to the phases ($k = g$ or $k = l$). α_k is the volume fraction ($\alpha_g + \alpha_l = 1$), ρ_k the density, $\overrightarrow{V_k}$ the velocity, e_k the energy, p_k the pressure and h_k the enthalpy ($h_k = e_k + \frac{p_k}{\rho_k}$). Moreover p_k^i, h_k^i and $\overrightarrow{V_k^i}$ refer respectively to the

pressure, the enthalpy and the velocity defined over the gas-liquid interface. The enthalpy equation is derived from the system above :

- **enthalpy conservation equation :**

$$\begin{aligned} \partial_t(\alpha_k\rho_k h_k) + \nabla.(\alpha_k\rho_k h_k\overrightarrow{V_k}) = Q_k^i + \Gamma_k h_k^i + \alpha_k D_t^k p_k + \\ (\overrightarrow{F_k^i} - (p_k - p_k^i)\nabla\alpha_k - \Gamma_k\overrightarrow{V_k}) \,.\, (\overrightarrow{V_k^i} - \overrightarrow{V_k}) \,, \end{aligned} \tag{4}$$

with

$$D_t^k p_k = \partial_t p_k + \overrightarrow{V_k}.\nabla p_k \,.$$

2.2 The closure relations

We refer to [4] and [1][11][12] for the details of the closure modelings. These modelings concern the source terms (the interphase drag force $\overrightarrow{F_k^i}$, the interfacial heat transfert Q_k^i and the mass transfert Γ_k) and the pressure fluctuation p_k^i. Finally a perfect gas law is used as equation of state for the gas pressure, the liquid being assumed to be incompressible.

3 The three dimensional model

3.1 The system of equations

We extend to the three dimensions of space the simplified two-fluid model presented in [4] for the two dimension of space. The velocity of the phase k is written as :

$$\overrightarrow{V_k} = (u_k, v_k, w_k)^{\mathrm{T}} \,. \tag{5}$$

and the model can be written under the following form :

$$\begin{aligned} &\partial_t W + \partial_x F(W) + \partial_y G(W) + \partial_z H(W) + \\ &A(W)\partial_x W + B(W)\partial_y W + C(W)\partial_z W = S(W) \end{aligned} \tag{6}$$

The details of the vector W, of the terms $S(W)$, $F(W)$, $G(W)$, $H(W)$, and of the matrices $A(W)$, $B(W)$, $C(W)$ are given in the appendix A.

The source terms closure modellings for

- the interfacial friction $\overrightarrow{F_k^i} = (F_{kx}^i, F_{ky}^i, F_{kz}^i)^{\mathrm{T}}$,
- the mass transfert Γ and the heat transfert Q_k^i,

are also 3D extensions of the ones presented in [4] in 2D. The details about the physical closure laws can be found in [1].

3.2 Eigenvalues and eigenvectors

We build a Roe flux scheme using approximate forms of the eigenvalues and of the eigenvectors. For this purpose we apply the density perturbation method presented in [3]. This approach is based on a scaling of the densities :

$$\rho_g \rightarrow \frac{\rho_g}{\rho_g^o} \, , \, \rho_l \rightarrow \frac{\rho_l}{\rho_l^o} \, ,$$

where ρ_g^o and ρ_l^o are two average densities and we will consider $\varepsilon = \frac{\rho_g^o}{\rho_l^o}$ the average density ratio. Following the work presented in [4], we write :

$$V_l^n = u_l n_x + v_l n_y + w_l n_z \tag{7}$$

and the Jacobian matrix of the conservative part of the two-fluid system at order zero writes [4] :

$$J = \begin{pmatrix} J_l & 0 \\ 0 & J_g \end{pmatrix} , \tag{8}$$

The details of the Jacobian matrix J and of its eigenvalues and its eigenvectors are given in the appendix B.

These formulas allow to explicitly compute the numerical flux associated with the full two-fluid model following the perturbation method [3].

4 The numerical scheme

We approximate the solution W of (6) on each cell Ω_i by :

$$W_i(t) \simeq \frac{1}{|\Omega_i|} \int_{\Omega_i} W(x,y,z,t) dx dy dz$$

and under the C.F.L. condition :

$$\frac{dt\, C}{|\Omega_i|} \sum_j |\Gamma_{ij}| \leq 1 \; ; \; \forall \Omega_i \in \Omega \tag{9}$$

the scheme writes

$$W_i^{t+dt} = W_i^t - \frac{dt}{|\Omega_i|} \sum_j |\Gamma_{ij}| \Phi(W_i^t, W_j^t, n_{ij}) + dt\, S(W_i^t)$$
$$- \frac{dt}{|\Omega_i|} \sum_j |\Gamma_{ij}| \left\{ A(W_i^t) n_{ij,x} + B(W_i^t) n_{ij,y} + C(W_i^t) n_{ij,z} \right\} W_{ij}^t \, . \tag{10}$$

More exactly,

- The convective conservative part is computed by the explicit Roe flux scheme $\Phi(W_i^t, W_j^t, n_{ij})$.
- A predicted step on the gradients is used to evaluate the non conservative products.
- Finaly, without steep coefficients, the source terms $S(W_i^t)$ are explicitly computed on each cell.

In the reference [4] more details are given about the benefits and the drawbacks of this method, and about the existence of other ways of doing.

5 Numerical results

There exists very few three dimensional test cases for the analysis of two-fluid systems for transient two-phase flows. Let us cite some very interesting proposals in [2] and [10]. In this work we have studied a new 3D test case whose validation is based on mesh refinements and on the physical consistency of the results.

5.1 Test case definition

The test case is a three dimensional generalization of the one dimensional experiment CANON ([13]). This is a pressure blowdown in a bended tube.
The radius of the tube section is $15\,cm$ and the total length of the tube is $160\,cm$. The tube geometry presents a 90^O bend (cf Fig. C.1). At the initial state the tube is full of liquid. The initial pressure is $58.10^5 Pa$ and the initial temperature is $515K$. This pressure is $21.10^5 Pa$ less than the saturated liquid pressure. The physical coefficients of the closure laws for the source terms are the same as the two dimensional blowdown presented in [4]. The other initial conditions are :

$$\begin{aligned} &\alpha_l = 0.99 && , \rho_g = 63\ (kg/m^3) \\ &u_g = v_g = w_g = 0\ (m/s) && , u_l = v_l = w_l = 0\ (m/s)\ \cdot \\ &h_g = 2798924\ (J/kg) && , h_l = 960790\ (J/kg) \end{aligned} \tag{11}$$

At the time $t = 0\ sec$, the bottom outlet of the tube is open to the atmospheric pressure ($10^5 Pa$). Then the fluid inside the tube starts to vaporize.

5.2 The meshes of the test case

A first coarse mesh is built with 2208 hexahedrons (7040 faces). Then, for the purpose of numerical validation, a second refined mesh is built with 17664 hexahedrons (54656 faces). This meshes are shown on the figure C.1.

5.3 Results

The C.F.L. condition (9) implies a time step $dt = 0.000012\,sec$ on the coarse mesh and $dt = 0.000006\,sec$ on the fine mesh. The computation with the fine mesh on a Intel Pentium IV 2 Ghz take 7 secondes per time step.

Following the opening of the tube, the pressure is decreasing fastly ([13]). We present the evolution of the void fraction, of the module of the relative velocity and of the pressure at $t = 24\,10^{-3}$, $48\,10^{-3}$, $72\,10^{-3}$ *et* $84\,10^{-3}\,sec$.
The figures C.2 and C.3 show the void fraction. The figures C.4 and C.5 show the module of the relative velocity. The figures C.6 and C.7 show the pressure.

- We have checked that the solution is stable with a mesh refinement. The volume

of a fine mesh cell is $\frac{1}{8}$ the volume of a coarse mesh cell.

- As it can be seen on the figure C.7 there is a low pressure area close to the inner side of the bend. In this area it can be observed large values of the module of the relative velocity (figure C.5). The gas, having a smaller density than the liquid, is subject to a larger acceleration in the depression area and larger values of the void fraction are also observed at the same place (figure C.3).
- The time evolution of the maximum value of the void fraction is presented on the figure C.8. The computation has been stopped just before this value reaches one.
- Trajectories of a gas particle and of a liquid particle are plotted on the figure C.9 and show an other effect of the density difference as the flow turns in the bend.
- In spite of the lack of experimental results this numerical simulation shows physicaly coherent results from a phenomenological point of view.

6 Conclusion

It has been shown that the density perturbation method can be extended to three dimensional transient two-phase flows analysis. As there are very few three dimensional results concerning real two phase flows, the flow studied in this paper would be an interesting proposal for testing two-phase flows computing method in 3D.

A Detailed terms of the equations

We recall the system of equations (6) :

$$\begin{aligned} &\partial_t W + \partial_x F(W) + \partial_y G(W) + \partial_z H(W) + \\ &A(W)\partial_x W + B(W)\partial_y W + C(W)\partial_z W = S(W) \end{aligned} \tag{A.1}$$

with

$$W = \begin{bmatrix} \alpha_l \rho_l \\ \alpha_l \rho_l u_l \\ \alpha_l \rho_l v_l \\ \alpha_l \rho_l w_l \\ \alpha_l \rho_l h_l \\ \alpha_g \rho_g \\ \alpha_g \rho_g u_g \\ \alpha_g \rho_g v_g \\ \alpha_g \rho_g w_g \\ \alpha_g \rho_g h_g \end{bmatrix}, \; S(W) = \begin{bmatrix} \Gamma_l \\ F^i_{lx} + \alpha_l \rho_l g_x \\ F^i_{ly} + \alpha_l \rho_l g_y \\ F^i_{lz} + \alpha_l \rho_l g_z \\ \Gamma h^s_l + Q^i_l \\ \Gamma_g \\ F^i_{gx} + \alpha_g \rho_g g_x \\ F^i_{gy} + \alpha_g \rho_g g_y \\ F^i_{gz} + \alpha_g \rho_g g_z \\ \Gamma h^s_g + Q^i_g \end{bmatrix},$$

and

$$F(W) = \begin{bmatrix} \alpha_l \rho_l u_l \\ \alpha_l \rho_l (u_l^2 + \theta) + \alpha_l P \\ \alpha_l \rho_l u_l v_l \\ \alpha_l \rho_l u_l w_l \\ \alpha_l \rho_l u_l h_l \\ \alpha_g \rho_g u_g \\ \alpha_g \rho_g u_g^2 + \alpha_g P \\ \alpha_g \rho_g u_g v_g \\ \alpha_g \rho_g u_g w_g \\ \alpha_g \rho_g u_g h_g \end{bmatrix}, \; G(W) = \begin{bmatrix} \alpha_l \rho_l v_l \\ \alpha_l \rho_l v_l u_l \\ \alpha_l \rho_l (v_l^2 + \theta) + \alpha_l P \\ \alpha_l \rho_l v_l w_l \\ \alpha_l \rho_l v_l h_l \\ \alpha_g \rho_g v_g \\ \alpha_g \rho_g v_g u_g \\ \alpha_g \rho_g v_g^2 + \alpha_g P \\ \alpha_g \rho_g v_g w_g \\ \alpha_g \rho_g v_g h_g \end{bmatrix}$$

and

$$H(W) = \begin{bmatrix} \alpha_l \rho_l w_l \\ \alpha_l \rho_l w_l u_l \\ \alpha_l \rho_l w_l v_l \\ \alpha_l \rho_l (w_l^2 + \theta) + \alpha_l P \\ \alpha_l \rho_l h_l \\ \alpha_g \rho_g w_g \\ \alpha_g \rho_g w_g u_g \\ \alpha_g \rho_g w_g v_g \\ \alpha_g \rho_g w_g^2 + \alpha_g P \\ \alpha_g \rho_g w_g h_g \end{bmatrix}.$$

the matrices $A(W)$, $B(W)$ and $C(W)$ are given by :

$$A = \begin{bmatrix} 0 & 0\,0\,0\,0\,0\,0\,0\,0\,0 \\ -\frac{1}{\rho_l}P & 0\,0\,0\,0\,0\,0\,0\,0\,0 \\ 0 & 0\,0\,0\,0\,0\,0\,0\,0\,0 \\ 0 & 0\,0\,0\,0\,0\,0\,0\,0\,0 \\ 0 & 0\,0\,0\,0\,0\,0\,0\,0\,0 \\ 0 & 0\,0\,0\,0\,0\,0\,0\,0\,0 \\ \frac{1}{\rho_l}P & 0\,0\,0\,0\,0\,0\,0\,0\,0 \\ 0 & 0\,0\,0\,0\,0\,0\,0\,0\,0 \\ 0 & 0\,0\,0\,0\,0\,0\,0\,0\,0 \\ 0 & 0\,0\,0\,0\,0\,0\,0\,0\,0 \end{bmatrix},$$

$$B = \begin{bmatrix} 0 & 0\ 0\ 0\ 0\ 0\ 0\ 0\ 0\ 0 \\ 0 & 0\ 0\ 0\ 0\ 0\ 0\ 0\ 0\ 0 \\ -\frac{1}{\rho_l}P & 0\ 0\ 0\ 0\ 0\ 0\ 0\ 0\ 0 \\ 0 & 0\ 0\ 0\ 0\ 0\ 0\ 0\ 0\ 0 \\ 0 & 0\ 0\ 0\ 0\ 0\ 0\ 0\ 0\ 0 \\ 0 & 0\ 0\ 0\ 0\ 0\ 0\ 0\ 0\ 0 \\ 0 & 0\ 0\ 0\ 0\ 0\ 0\ 0\ 0\ 0 \\ \frac{1}{\rho_l}P & 0\ 0\ 0\ 0\ 0\ 0\ 0\ 0\ 0 \\ 0 & 0\ 0\ 0\ 0\ 0\ 0\ 0\ 0\ 0 \\ 0 & 0\ 0\ 0\ 0\ 0\ 0\ 0\ 0\ 0 \end{bmatrix},$$

$$C = \begin{bmatrix} 0 & 0\ 0\ 0\ 0\ 0\ 0\ 0\ 0\ 0 \\ 0 & 0\ 0\ 0\ 0\ 0\ 0\ 0\ 0\ 0 \\ 0 & 0\ 0\ 0\ 0\ 0\ 0\ 0\ 0\ 0 \\ -\frac{1}{\rho_l}P & 0\ 0\ 0\ 0\ 0\ 0\ 0\ 0\ 0 \\ 0 & 0\ 0\ 0\ 0\ 0\ 0\ 0\ 0\ 0 \\ 0 & 0\ 0\ 0\ 0\ 0\ 0\ 0\ 0\ 0 \\ 0 & 0\ 0\ 0\ 0\ 0\ 0\ 0\ 0\ 0 \\ 0 & 0\ 0\ 0\ 0\ 0\ 0\ 0\ 0\ 0 \\ \frac{1}{\rho_l}P & 0\ 0\ 0\ 0\ 0\ 0\ 0\ 0\ 0 \\ 0 & 0\ 0\ 0\ 0\ 0\ 0\ 0\ 0\ 0 \end{bmatrix}.$$

B Details on the eigenvalues and the eigenvectors

The terms of the Jacobian matrix (8) are :

$$J_l = \begin{pmatrix} 0 & n_x & n_y & n_z & 0 \\ -u_l V_l^n + \theta n_x & u_l n_x + V_l^n & u_l n_y & u_l n_z & 0 \\ -v_l V_l^n + \theta n_y & v_l n_x & v_l n_y + V_l^n & v_l n_z & 0 \\ -w_l V_l^n + \theta n_z & w_l n_x & w_l n_y & w_l n_z + V_l^n & 0 \\ -h_l V_l^n & h_l n_x & h_l n_y & h_l n_z & V_l^n \end{pmatrix} \tag{B.1}$$

and

$$J_g = \begin{pmatrix} 0 & n_x & n_y & n_z & 0 \\ -u_g V_g^n & u_g n_x + V_g^n & u_g n_y & u_g n_z & \frac{\gamma-1}{\gamma} n_x \\ -v_g V_g^n & v_g n_x & v_g n_y + V_g^n & v_g n_z & \frac{\gamma-1}{\gamma} n_y \\ -w_g V_g^n & w_g n_x & w_g n_y & w_g n_z + V_g^n & \frac{\gamma-1}{\gamma} n_z \\ -h_g V_g^n & h_g n_x & h_g n_y & h_g n_z & V_g^n \end{pmatrix} \tag{B.2}$$

We develop this Jacobian matrix in eigen elements :

$$J_k = P_k D_k P_k^{-1} \, , \tag{B.3}$$

with

$$D_l = \begin{pmatrix} V_l^n & 0 & 0 & 0 & 0 \\ 0 & V_l^n & 0 & 0 & 0 \\ 0 & 0 & V_l^n & 0 & 0 \\ 0 & 0 & 0 & V_l^n - \sqrt{\theta} & 0 \\ 0 & 0 & 0 & 0 & V_l^n + \sqrt{\theta} \end{pmatrix}, \tag{B.4}$$

$$D_g = \begin{pmatrix} V_g^n & 0 & 0 & 0 & 0 \\ 0 & V_g^n & 0 & 0 & 0 \\ 0 & 0 & V_g^n & 0 & 0 \\ 0 & 0 & 0 & V_g^n - \sqrt{\frac{\partial P}{\partial \rho_g}} & 0 \\ 0 & 0 & 0 & 0 & V_g^n + \sqrt{\frac{\partial P}{\partial \rho_g}} \end{pmatrix}, \tag{B.5}$$

for $n_x \neq 0$:

$$P_g = \begin{pmatrix} 1 & 0 & 0 & 1 & 1 \\ u_g & -n_y & -n_z & u_g - \sqrt{\frac{\partial P}{\partial \rho_g}} n_x & u_g + \sqrt{\frac{\partial P}{\partial \rho_g}} n_x \\ v_g & n_x & 0 & v_g - \sqrt{\frac{\partial P}{\partial \rho_g}} n_y & v_g + \sqrt{\frac{\partial P}{\partial \rho_g}} n_y \\ w_g & 0 & n_x & w_g - \sqrt{\frac{\partial P}{\partial \rho_g}} n_z & w_g + \sqrt{\frac{\partial P}{\partial \rho_g}} n_z \\ 0 & 0 & 0 & h_g & h_g \end{pmatrix}, \tag{B.6}$$

$$P_l = \begin{pmatrix} 0 & 0 & 0 & 1 & 1 \\ 0 & -n_y & -n_z & u_l - \sqrt{\theta} n_x & u_l + \sqrt{\theta} n_x \\ 0 & n_x & 0 & v_l - \sqrt{\theta} n_y & v_l + \sqrt{\theta} n_y \\ 0 & 0 & n_x & w_l - \sqrt{\theta} n_z & w_l + \sqrt{\theta} n_z \\ 1 & 0 & 0 & h_l & h_l \end{pmatrix}, \tag{B.7}$$

for $n_y \neq 0$:

$$P_g = \begin{pmatrix} 1 & 0 & 0 & 1 & 1 \\ u_g & n_y & 0 & u_g - \sqrt{\frac{\partial P}{\partial \rho_g}} n_x & u_g + \sqrt{\frac{\partial P}{\partial \rho_g}} n_x \\ v_g & -n_x & -n_z & v_g - \sqrt{\frac{\partial P}{\partial \rho_g}} n_y & v_g + \sqrt{\frac{\partial P}{\partial \rho_g}} n_y \\ w_g & 0 & n_y & w_g - \sqrt{\frac{\partial P}{\partial \rho_g}} n_z & w_g + \sqrt{\frac{\partial P}{\partial \rho_g}} n_z \\ 0 & 0 & 0 & h_g & h_g \end{pmatrix}, \tag{B.8}$$

$$P_l = \begin{pmatrix} 0 & 0 & 0 & 1 & 1 \\ 0 & n_y & 0 & u_l - \sqrt{\theta} n_x & u_l + \sqrt{\theta} n_x \\ 0 & -n_x & -n_z & v_l - \sqrt{\theta} n_y & v_l + \sqrt{\theta} n_y \\ 0 & 0 & n_y & w_l - \sqrt{\theta} n_z & w_l + \sqrt{\theta} n_z \\ 1 & 0 & 0 & h_l & h_l \end{pmatrix}, \tag{B.9}$$

for $n_z \neq 0$:

$$P_g = \begin{pmatrix} 1 & 0 & 0 & 1 & 1 \\ u_g & n_z & 0 & u_g - \sqrt{\frac{\partial P}{\partial \rho_g}} n_x & u_g + \sqrt{\frac{\partial P}{\partial \rho_g}} n_x \\ v_g & 0 & n_z & v_g - \sqrt{\frac{\partial P}{\partial \rho_g}} n_y & v_g + \sqrt{\frac{\partial P}{\partial \rho_g}} n_y \\ w_g & -n_x & -n_y & w_g - \sqrt{\frac{\partial P}{\partial \rho_g}} n_z & w_g + \sqrt{\frac{\partial P}{\partial \rho_g}} n_z \\ 0 & 0 & 0 & h_g & h_g \end{pmatrix}, \tag{B.10}$$

$$P_l = \begin{pmatrix} 0 & 0 & 0 & 1 & 1 \\ 0 & n_z & 0 & u_l - \sqrt{\theta} n_x & u_l + \sqrt{\theta} n_x \\ 0 & 0 & n_z & v_l - \sqrt{\theta} n_y & v_l + \sqrt{\theta} n_y \\ 0 & -n_x & -n_y & w_l - \sqrt{\theta} n_z & w_l + \sqrt{\theta} n_z \\ 1 & 0 & 0 & h_l & h_l \end{pmatrix}. \tag{B.11}$$

C Figures

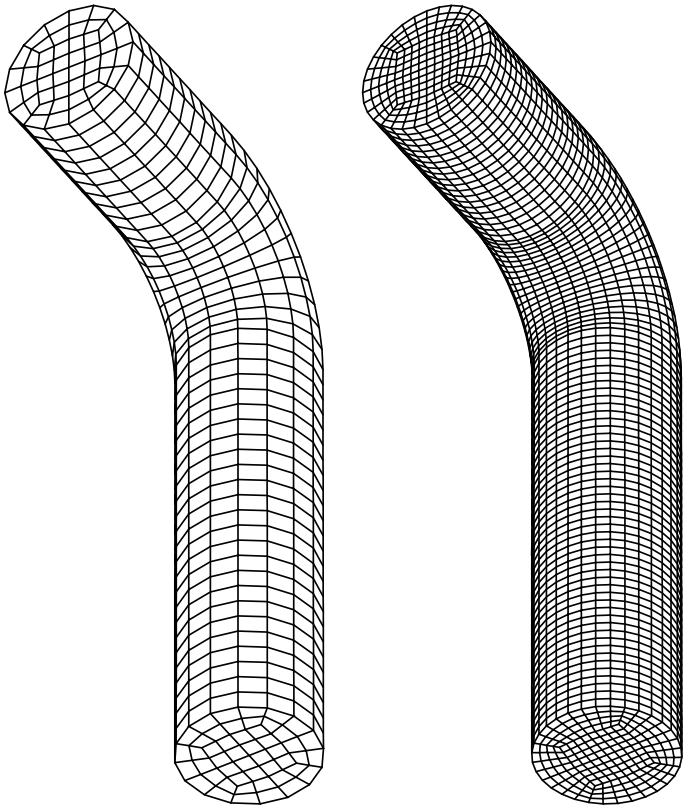

Fig. C.1. Coarse and refined meshes of the bended tube

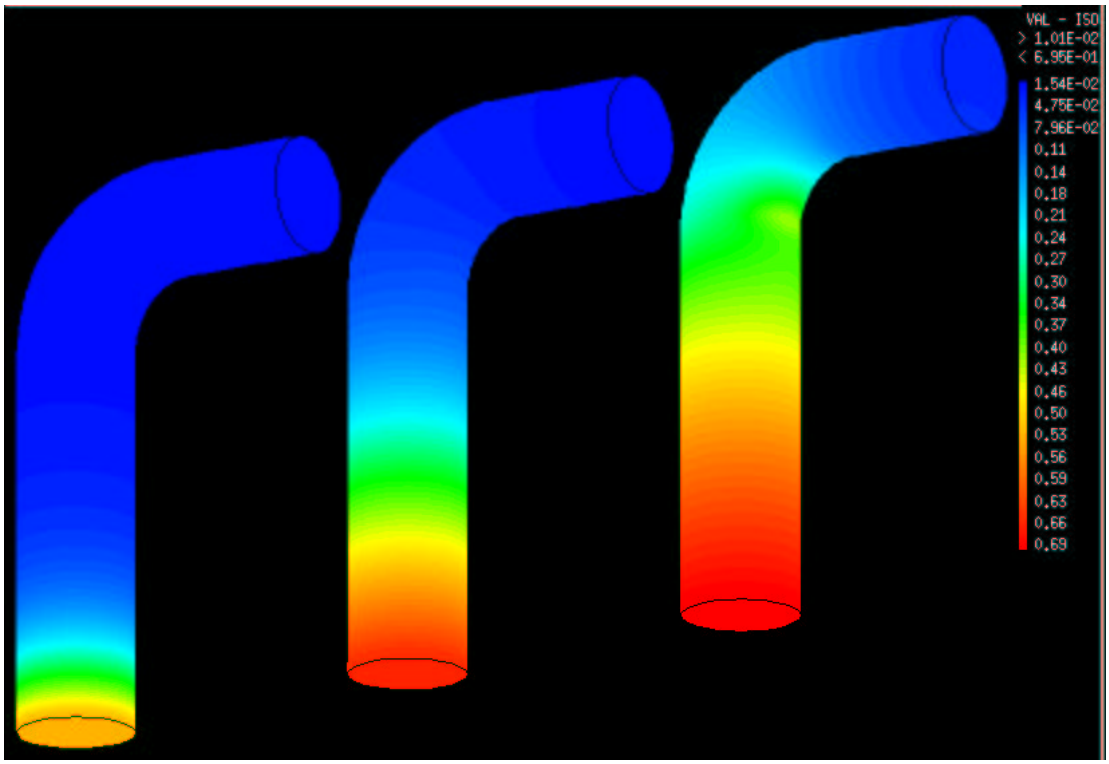

Fig. C.2. Void fraction at time 24, 48, 72 ms

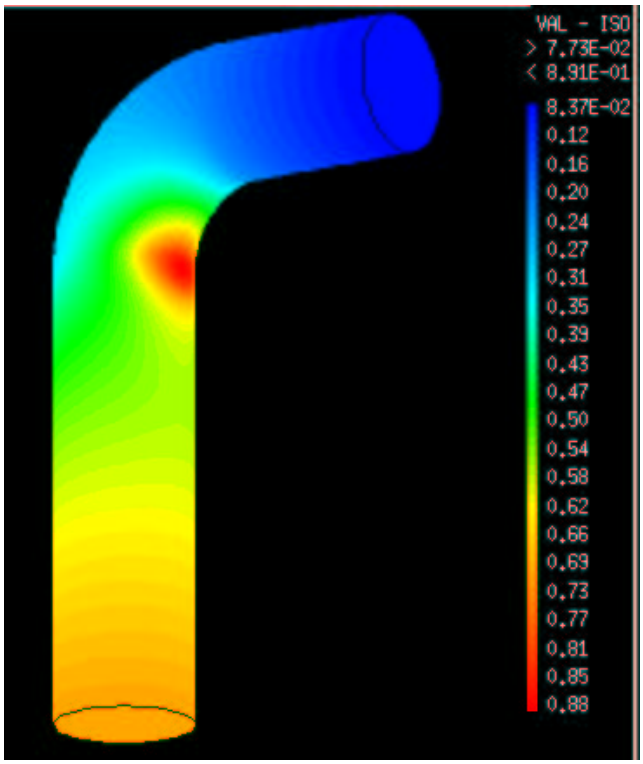

Fig. C.3. Void fraction at time 84 ms

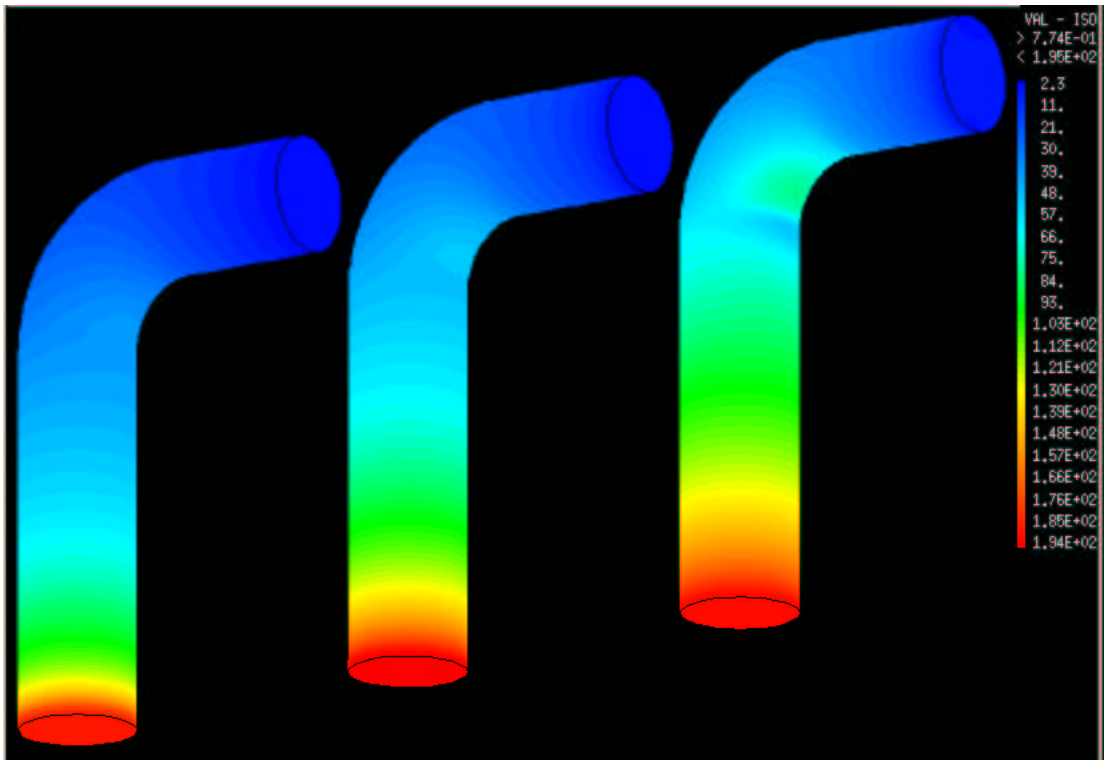

Fig. C.4. Relative velocity at time 24, 48, 72 ms

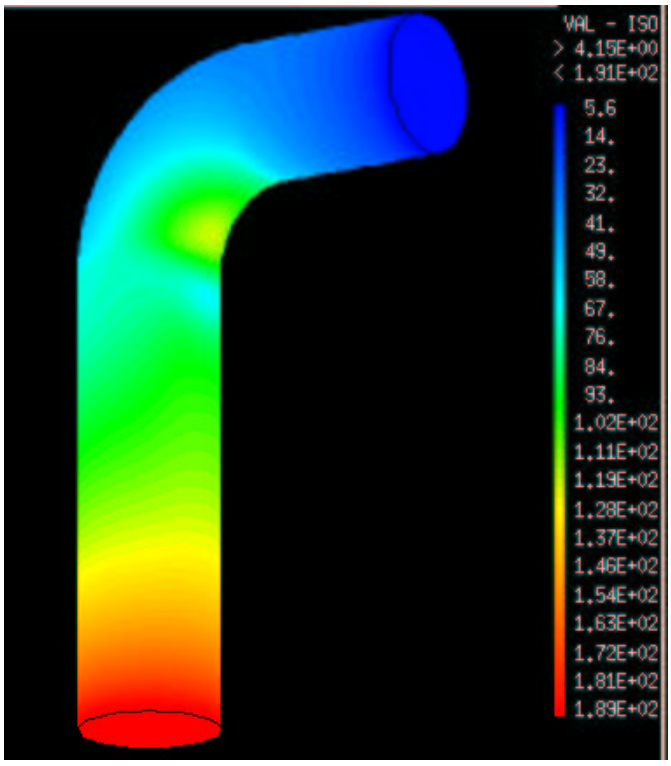

Fig. C.5. Relative velocity at time 84 ms

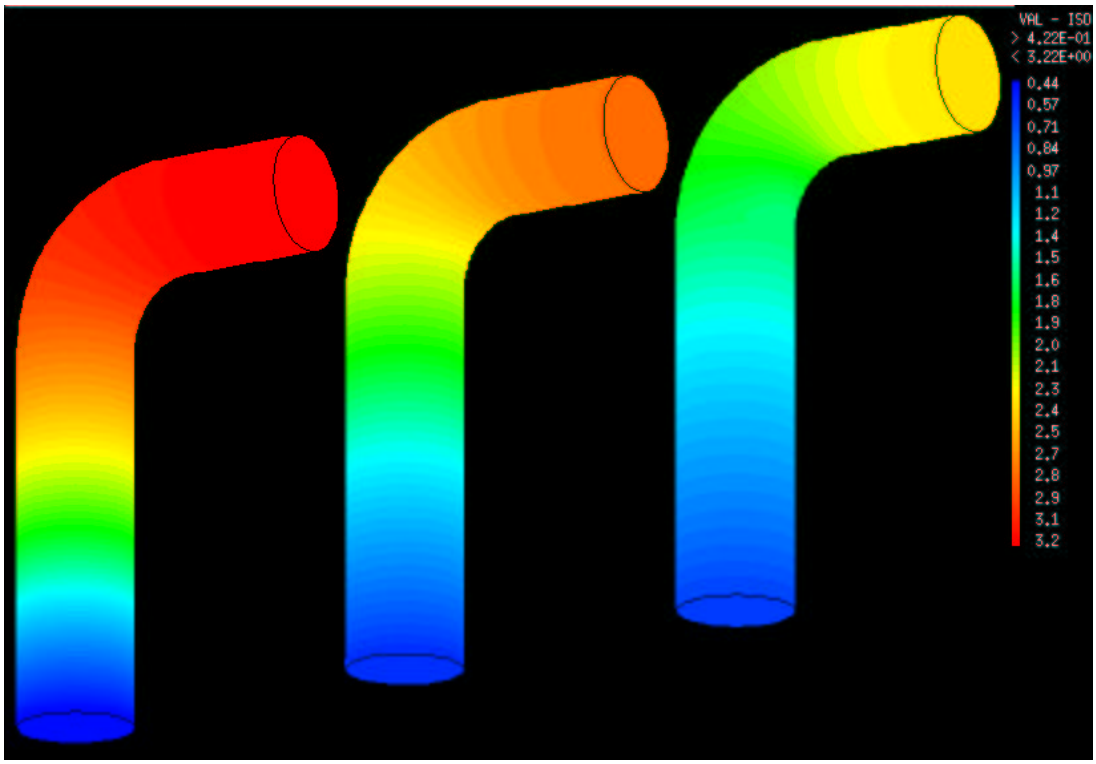

Fig. C.6. Pressure at time 24, 48, 72 ms

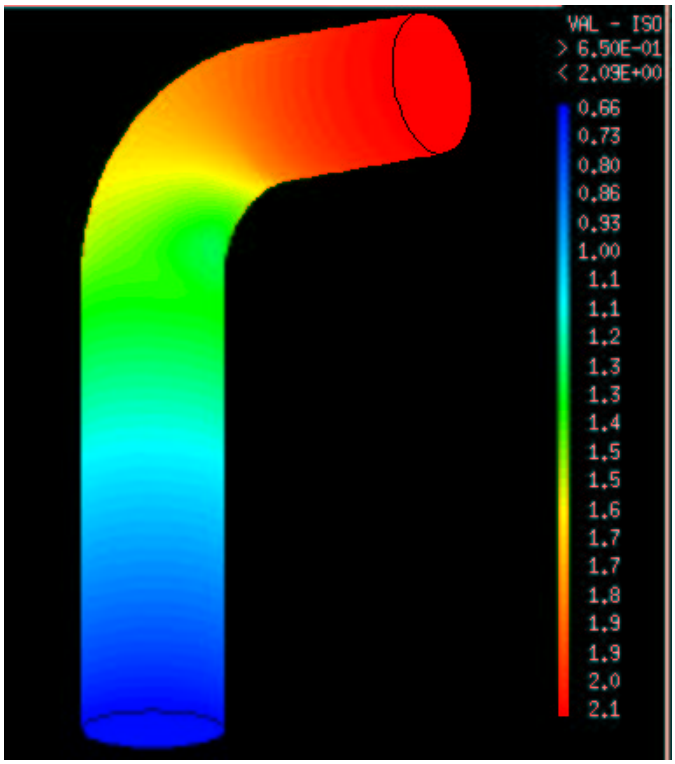

Fig. C.7. Pressure at time 84 ms

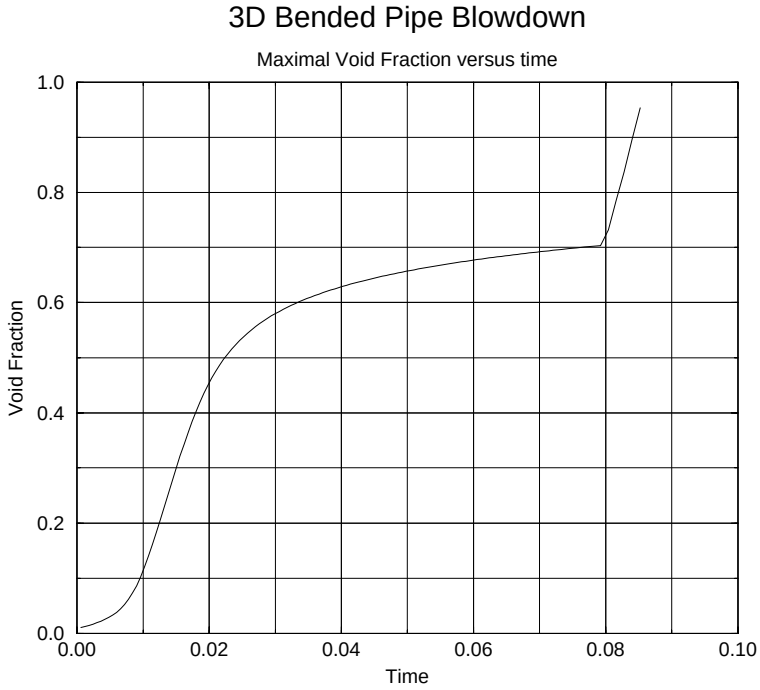

Fig. C.8. Time evolution of the void fraction maximum value

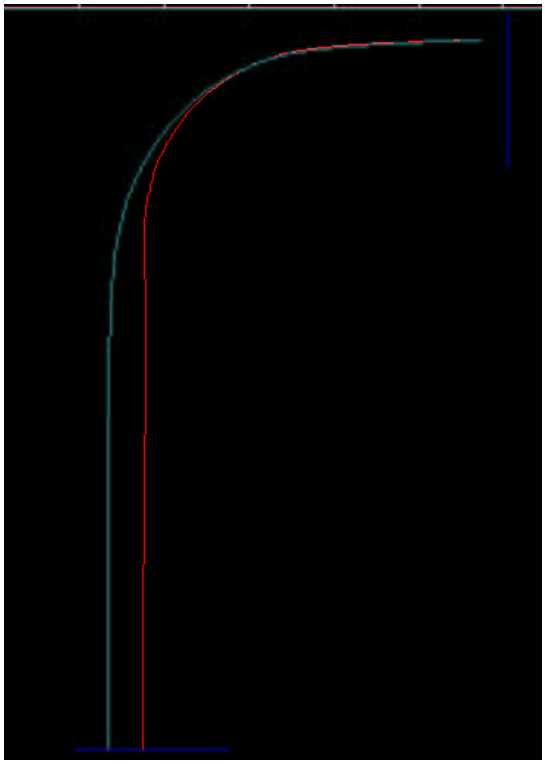

Fig. C.9. Liquid and gas trajectories

References

[1] D. BESTION, *The physical closure laws in the Cathare code*, Nuclear Engineering and Design, Vol.124, 1990, pp. 229–245

[2] M. BOUCKER, *Modélisation numérique multidimensionnelle d'écoulements diphasiques liquide-gaz en régimes transitoire et permanent : méthodes et applications*, PhD thesis at Ecole Normale Supérieure de Cachan, June 1998

[3] J. CORTES, A. DEBUSSCHE AND I. TOUMI, *A Density Perturbation Method to study the Eigenstructure of Two-Phase Flow Equation Systems*, Journal of Computational Physics, Vol.147, No.2, 1998, pp. 463–484

[4] J. CORTES, *On the construction of upwind schemes for non-equilibrium transient two-phase flows*, Computers & Fluids 31(2002):159-182

[5] J. M. DELHAYE, M. GIOT AND M. L. RIETHMULLER, *Thermohydraulics of Two-Phase Systems for Industrial Design and Nuclear Engineering*, Von Karman Institute, Mc Graw Hill Book Compagny, 1981

[6] M. ISHII, *Thermo-Fluid Dynamic Theory of Two-Phase Flow*, Eyrolles, Paris, 1975

[7] J.M. GHIDAGLIA, *Numerical computation of three dimensional two-phase flows by finite volumes methods using flux schemes*, Finite Volumes in Complex Applications, Duisburg, Germany, 1999

[8] J.M. GHIDAGLIA, G. LECOQ, I. TOUMI, *Two flux schemes for computing two-phase flows through multidimensional finite volumes methods*, 9th Int. Topical Meeting on Nuclear Reactor Thermal Hydraulic, San Francisco, USA, October 1999

[9] E. LORIN, *Sur la stabilité de modèles pour la mécanique des fluides numérique dans le contexte volumes finis*, Thèse, ENS Cachan, 2001

[10] S. KORTAS AND D. BESTION, *Propositions de benchmarks physiques et numériques en diphasique*, Ecoulements compressibles et Mécanique des fluides numérique, XI séminaire, CEA Saclay, Janvier 99

[11] R. T. LAHEY, JR., *The prediction of phase distribution and separation phenomena using two-fluid models*, Boiling Heat Transfert, Elsevier Science Publishers, 1992, pp. 85–121

[12] S. J. LEE, K. S. CHANG AND K. KIM, *Pressure wave speed from the characteristics of two fluids, two-phase hyperbolic equation system*, International Journal of Multiphase Flow, Vol.24, 1998, pp. 855–866

[13] J. C. ROUSSEAU, *Blowdown* , Multiphase Science and Technology, Vol.3, G.F.Hewitt and J.M.Delhaye and N.Zuber, Hemisphere Publishing Corporation, 1987, pp. 442–449.

[14] H. STADTKE, G. FRONCHELLO AND B. WORTH, *Numerical simulation of multidimensional two-phase flow based on flux vector splitting*, Nuclear Engineering and Design,Vol.177, 1997, pp. 199-213